JEE Journal of Ecological Engineering

Journal of Ecological Engineering, 2026, 27(6), 14–29
https://doi.org/10.12911/22998993/215517
ISSN 2299–8993, License CC-BY 4.0

Received: 2025.12.06
Accepted: 2026.04.16
Published: 2026.05.01

Synthesis and characterization of ethylenediamine and cupric ions functionalized fly-ash silica xerogel and ANN-based prediction of its heavy metal adsorption performance

Edi Nasra[1,2], Deswati[1*], Safni[1], Yulia Eka Putri[1], M. Iqbal Saputra Gemasih[2], Adewirli Putra[3]

[1] Department of Chemistry, Faculty of Mathematics Natural Sciences, Andalas University, Padang, Indonesia
[2] Department of Chemistry, Faculty of Mathematics Sciences, Universitas Negeri Padang, Padang, Indonesia
[3] Department of Medical Laboratory Technology, Syedza Saintika University, Padang, Indonesia
* Corresponding author's e-mail: deswati@sci.unand.ac.id

ABSTRACT

Silica xerogel derived from fly ash was synthesized and subsequently functionalized with ethylenediamine (EDA) and cupric ions (Cu^{2+}) to produce a renewable hybrid adsorbent (SiO_2@NH_2–Cu) aimed at enhancing heavy metal removal from aqueous systems. The integrated process – comprising acid leaching, alkaline extraction, sol-gel gelation, and sequential organic/metal functionalization – successfully transformed crystalline fly ash into a high-purity amorphous silica framework. Acid activation increased the SiO_2 content from 32.867 to 46.016 mg/kg, while the final xerogel achieved 71.053 mg/kg, confirming efficient impurity removal and silica enrichment. Fourier transform infrared (FTIR) analysis verified the incorporation of –NH_2 and –CH_2 groups, while energy dispersive X-ray spectroscopy (EDS) revealed 0.46 wt% Cu, indicating effective metal anchoring onto the amine-functionalized silica surface. Textural analysis showed a mesoporous architecture with a surface area of 77.42 m^2/g, a pore volume of 0.3894 cm^3/g, and an average pore diameter of 16.09 nm, demonstrating substantial pore expansion following functionalization. Field emission scanning electron microscopy (FESEM) imaging further revealed uniform morphology and homogeneous Cu distribution. An artificial neural network (ANN) model was developed to predict adsorption performance based on structural and surface chemistry parameters, including pore size, –NH_2 group density, and Cu loading. Sensitivity analysis confirmed these parameters as the dominant contributors to adsorption efficiency. The combined experimental–computational approach highlights the synergistic role of EDA and Cu^{2+} in enhancing surface reactivity, establishing SiO_2@NH_2–Cu as a promising low-cost, sustainable adsorbent for wastewater treatment and related environmental applications.

Keywords: adsorbent, ANN prediction, ethylenediamine, fly ash, silica xerogel.

INTRODUCTION

The rapid growth of global industrialization has inevitably increased the generation of solid waste, including fly ash, which is the residue produced from coal combustion in thermal power plants. Improper handling of fly ash poses significant risks to both the environment and public health, due to its fine particle size, mobility, and potential for toxic metal leaching (Owoeye et al., 2020; Wang et al., 2015). In the context of global efforts to reduce carbon emissions and achieve carbon neutrality, developing effective and sustainable fly ash management strategies is imperative (Yang et al., 2024).

Traditionally, fly ash has been utilized in the production of bricks, cement, and concrete, as well as in agriculture to improve soil structure (Lewińska et al., 2024). However, the majority of fly ash remains underutilized and is often disposed of in landfills, contributing to secondary pollution as well as increasing long-term operational costs (Li and Wang, 2025). An alternative valorization strategy involves converting fly ash-derived silica into functional materials, particularly for environmental applications.

Silicon dioxide (SiO_2) is one of the most promising functional materials due to its high thermal stability, low cost, ease of modification, and natural abundance (Chang et al., 2025; Dolatabadi et al., 2023; Zheng et al., 2024). However, the surface of unmodified silica contains reactive silanol (–OH) groups, which are prone to condensation and aggregation, thereby limiting its performance in practical applications (Pilato et al., 2025; Souto and Machado, 2023). To overcome this, surface modification strategies, such as grafting organic functional groups are widely employed to enhance chemical stability and adsorption properties (Akti and Balci, 2023).

Recent trends in material science have focused on the development of organic–inorganic hybrid silica materials. These materials combine a silica framework with organic moieties that can interact through covalent or non-covalent bonding (Souto and Machado, 2023). Among the most commonly used synthesis techniques for hybrid materials is the sol–gel method, which allows for the incorporation of functional groups directly into the silica network during gelation (Kaya et al., 2021; Taleb et al., 2024). The sol–gel-derived silica materials are known for their high specific surface area, thermal and mechanical stability, as well as tunable pore structures, making them ideal candidates for applications in adsorption, catalysis, drug delivery, and sensing (Fan et al., 2025).

To further enhance the performance of silica-based adsorbents, surface functionalization techniques – such as co-condensation and post-synthesis grafting – have been developed. While each method has its merits, limitations still exist in terms of uniformity of functional group distribution and pore structure integrity (Abidli et al., 2025; Fernandes et al., 2019). In response, the use of amorphous, unpatterned xerogel-type silica synthesized via sol–gel routes has emerged as a promising alternative. Xerogels offer higher porosity and greater functional group loading capacity, yet remain underexplored for environmental applications (Das et al., 2021; Medina et al., 2023).

Incorporating amine functionalities ($–NH_2$) onto silica surfaces has been shown to significantly improve heavy metal adsorption due to their chelating ability (Fan et al., 2025). Furthermore, the introduction of transition metal ions, such as Cu^{2+}, provides dual active sites that enhance surface reactivity and broaden the range of adsorption capabilities. Accordingly, this study aimed to synthesize and characterize ethylenediamine and Cu^{2+}-modified silica xerogel ($SiO_2@NH_2–Cu$) as a novel hybrid adsorbent material. The specific objectives were: (1) to develop a sol–gel-based synthesis protocol for amorphous silica xerogel, (2) to sequentially graft ethylenediamine and impregnate Cu^{2+} ions onto the silica surface, (3) to characterize the structural as well as chemical features of the resulting material using spectroscopic and microscopic techniques, and (4) to evaluate its potential as a renewable, environmentally friendly adsorbent.

The novelty of this research lies in the dual-step surface modification strategy, involving ethylenediamine grafting followed by Cu^{2+} ion loading, which creates synergistic dual active sites for enhanced adsorption. To the best of authors' knowledge, this approach has not been widely reported, particularly in the context of utilizing fly ash-derived silica. In addition, an artificial neural network (ANN) model was developed to predict the adsorption performance based on structural, textural, and surface functionalization parameters, allowing optimization of key factors such as pore size distribution, $–NH_2$ density, and Cu^{2+} content. This work contributes not only to the advancement of functional hybrid materials but also to sustainable waste valorization practices by developing cost-effective, high-performance adsorbents guided by predictive modeling.

METHODOLOGY

Materials

The primary raw material used in this study was the fly ash was obtained from coal combustion in steam power plant. Fly ash is known to be rich in silica content, making it a potential raws material waste not only provides a sustainable source of silica but also supports circular economy approaches by minimizing environmental burden (Scherdel and Reichenauer, 2015). Distilled water was obtained from a Barnstead™ Smart2Pure™ Water Purification System (Thermo Fisher Scientific) at the Integrated Research Laboratory. Analytical-grade ethylenediamine ($NH_2CH_2CH_2NH_2$), hydrochloric acid (HCl), sodium hydroxide (NaOH), ethanol (C_2H_5OH), as well as copper(II) chloride dihydrate ($CuCl_2·2H_2O$) were purchased from Merck (Germany) and used without further purification.

Sample preparation

Silica xerogel was synthesized from fly ash using a modified sol–gel method, based on our previous study. Initially, the fly ash was incinerated to obtain ash, which was then acid-leached to remove inorganic contaminants and metallic impurities. Specifically, the ash was mixed with 3 M HCl at a ratio of 1:4 (w/v) and heated at 80 °C for 2 hours. The resulting suspension was filtered, washed with deionized water until neutral pH (pH 7) was reached, and subsequently dried at 105 °C in a drying oven.The acid-treated ash was used for sodium silicate (Na_2SiO_3) extraction by reacting it with 7 M NaOH at a solid-to-liquid ratio of 1:24 (w/v) at 80 °C for 1 hour under continuous stirring. The chemical reaction involved is shown in Equation 1:

$$xSiO_2 \text{ (in fly ash)} + 2NaOH \rightarrow \rightarrow Na_2O.xSiO_2 + H_2O \quad (1)$$

The sodium silicate solution was then gelled by the slow addition of 3 M HCl under constant stirring, leading to the formation of silica gel, as shown in Equation 2:

$$Na_2O.xSiO_2 + 2HCl \rightarrow xSiO_2 + 2NaCl + H_2O \quad (2)$$

The resulting silica gel was washed thoroughly with deionized water to remove residual Na^+ ions, then dried and stored for further modification. To introduce amine functional groups, the silica xerogel was modified using ethylenediamine via grafting. A mixture of silica and ethylenediamine (1:2 w/v) was stirred at 40 °C for 6 hours to promote surface interaction between the silanol groups and amine functionalities (Gaur et al., 2018; Megersa et al., 2025; Zhou et al., 2025). After modification, the material was washed with 96% ethanol to remove unreacted ethylenediamine and dried at 78 °C.

Subsequently, the amine-modified silica was impregnated with a 0.1 M $CuCl_2$ solution at a ratio of 1:1.5 (w/v) under stirring, followed by drying at 70°C. The impregnated material was then calcined in a muffle furnace at 400 °C for 4 hours to obtain the final product: Cu(II)-impregnated amine-functionalized silica xerogel (SiO_2@NH_2–Cu). The incorporation of Cu^{2+} ions is expected to enhance the adsorption capacity of the material via coordination bonding and redox reactivity, which are beneficial for environmental applications, such as wastewater treatment (Owoeye et al., 2020)

Fourier transform infrared spectroscopy

Fourier transform infrared (FTIR) spectroscopy was employed to investigate the surface functional groups of the raw fly ash and the synthesized adsorbent (SiO_2@NH_2-Cu). The analysis was performed using a ThermoScientific FTIR spectrometer, with spectra recorded in the wavenumber range of 400–4000 cm^{-1}. FTIR is a powerful technique for identifying specific chemical bonds through their characteristic vibrational frequencies. In the raw material, typical absorption bands associated with silanol (Si–OH), siloxane (Si–O–Si), and adsorbed water (H–O–H bending) were observed, indicating the presence of amorphous silica. After modification with ethylenediamine and $CuCl_2$, the FTIR spectra exhibited new peaks corresponding to N–H bending, C–N stretching, and potential Cu–N coordination bonds, confirming successful surface functionalization and metal incorporation (P. Wang et al., 2015). The comparative spectra provided insights into the chemical interactions between the functional groups and metal ions involved in the surface modification.

X-ray diffraction

X-ray diffraction (XRD) analysis was conducted to evaluate the crystalline or amorphous nature of the raw fly ash and the modified adsorbent. Measurements were carried out using a PANalytical X'PERT PRO POWDER diffractometer (model PW3040/60), with diffraction patterns recorded at a scanning angle (2θ) starting from 3°, under a maintained temperature of 70 °C. The raw fly ash exhibited a broad hump between 15°–30° (2θ), characteristic of amorphous silica phases, along with crystalline peaks attributed to mullite, quartz, and other mineral impurities commonly found in industrial fly ash (Eteba et al., 2023). After surface modification, additional peaks emerged, indicating the presence of copper-related phases, possibly $Cu(OH)_2$ or CuO, which are typically formed during copper complexation with amino-functionalized silica. The XRD patterns confirmed both the preservation of the amorphous silica framework and the successful deposition of copper species on the surface.

Brunauer-Emmett-Teller surface area analysis

The specific surface area, total pore volume, and average pore size distribution of the raw as well as modified materials were determined using

the Brunauer-Emmett-Teller (BET) nitrogen adsorption-desorption technique. The measurements were conducted on a NOVA 800 instrument (Quantachrome, USA), using a gas mixture of 22.9 mol% N_2 and 77.1 mol% He as the adsorbate and carrier gases. Prior to analysis, the samples were degassed under vacuum at 150 °C for 12 hours to remove physisorbed moisture. The BET surface area was calculated from the adsorption isotherm, while the Barrett-Joyner-Halenda (BJH) method was used to estimate pore size distribution. The raw fly ash exhibited relatively low surface area and pore volume, reflecting its compact structure. Upon functionalization with ethylenediamine and copper ions, a significant increase in both surface area and mesopore volume was observed, indicating enhanced textural properties suitable for adsorption applications (Yang et al., 2024). These improvements were attributed to the generation of additional surface sites and pore channels introduced during the sol–gel and metal-anchoring processes.

Field emission scanning electron microscopy and energy dispersive X-ray spectroscopy

The surface morphology and elemental composition of the samples were examined using field emission scanning electron microscopy (FESEM) coupled with energy dispersive X-ray spectroscopy (EDS). Imaging was performed using a ThermoScientific Quattro SEM instrument operated at 5.00 kV. Prior to analysis, all samples were coated with a thin layer of gold using a sputtering unit to prevent charging under the electron beam. The raw fly ash displayed heterogeneous particle sizes with irregular surfaces and dense agglomerates, typical of combustion residues. After surface functionalization, the morphology of SiO_2@NH_2-Cu showed a more porous and roughened texture, indicating structural changes due to silanization and copper anchoring. The EDS analysis confirmed the elemental composition of the materials, with strong signals corresponding to silicon (Si), oxygen (O), and aluminum (Al) in the raw material. In the modified adsorbent, additional peaks corresponding to nitrogen (N) and copper (Cu) were detected, further validating the successful grafting of amine groups and coordination with Cu^{2+} ions (Lewińska et al., 2024; Riyanto et al., 2025). These findings were in agreement with the FTIR, XRD, and BET analyses, providing holistic evidence of successful material transformation for adsorption purposes.

Artificial neural network procedure

An artificial neural network (ANN) model was developed to predict the adsorption performance of the ethylenediamine–Cu^{2+} functionalized silica xerogel (SiO_2@NH_2–Cu), capitalizing on the ability of ANN to model complex, nonlinear interactions between material properties and functional outcomes (Mahdi et al., 2021; Srivastava et al., 2024). Input features included structural, textural, chemical, and surface functionalization parameters, such as specific surface area, pore volume, average pore diameter, –NH_2 density, and Cu^{2+} content. Comprehensive characterization of the xerogel was conducted using complementary techniques: elemental composition (EDS and elemental analysis), crystallinity (XRD), textural properties (BET and BJH), surface functional groups (FTIR), and morphology (FESEM). Data preprocessing involved missing value imputation, normalization, and categorical transformation, followed by grouped k-fold cross-validation to ensure robust evaluation and prevent data leakage.

All data used for training and validating the ANN model were obtained exclusively from the experimental characterization results generated in this study, including BET/BJH textural parameters, FTIR functional group intensities, EDS-derived elemental composition, Cu loading, surface –NH_2 density, and morphological descriptors from FESEM analysis. No external datasets or literature-derived numerical data were used, ensuring that the ANN prediction fully reflects the empirical characteristics of the synthesized SiO_2@NH_2–Cu adsorbent.

The ANN architecture consisted of an input layer representing the measured features, two hidden layers capturing nonlinear relationships among pore structure, surface chemistry, and Cu^{2+} incorporation, and an output layer predicting adsorption capacity (mg/g) or removal efficiency (%). Hidden layers employed ReLU activation, dropout, and L2 regularization, while the output layer used a linear function for continuous prediction. Training was performed using backpropagation with the Adam optimizer, minimizing mean squared error (MSE).

Further methodological details regarding the ANN configuration were provided to enhance

transparency and reproducibility. The network was trained for 300 epochs with a batch size of 16, employing an 80:20 training–validation split. The two hidden layers contained 64 and 32 neurons, respectively, and were regularized using a dropout rate of 0.2 combined with L2 regularization ($\lambda = 0.001$) to mitigate overfitting. Optimization was performed using the Adam algorithm with mean squared error as the loss function. The training achieved a final MSE of 0.0028, while the validation dataset yielded an MSE of 0.0034, indicating stable convergence and strong generalization performance.

Sensitivity analysis highlighted pore size distribution, $–NH_2$ density, and Cu^{2+} content as the most influential factors, in line with the prior studies emphasizing mesoporosity and surface functionalities in metal ion adsorption (Da'na, 2017; de Souza et al., 2019). This ANN framework provides a reliable predictive tool for designing functionalized silica xerogels and optimizing synthesis conditions to maximize environmental remediation efficiency.

RESULTS AND DISCUSSION

The silica (SiO_2) content in various samples is summarized in Table 1. Raw fly ash (FA), used as the precursor material, exhibited a silica content of 32.867 mg/kg. After acid washing with hydrochloric acid (HCl), the silica content significantly increased to 46,016 mg/kg, indicating the effective removal of inorganic impurities such as Fe, Al, and Ca. This purification step enhanced the reactive silica fraction in the material. For comparison, pure commercial silica demonstrated a SiO_2 content of 71.053 mg/kg. Although the acid-treated FA exhibited a lower silica content than pure silica, the improvement was substantial, confirming its potential as a sustainable precursor for silica-based materials. These findings align with prior studies reporting that acid activation improves silica recovery from aluminosilicate industrial wastes (Chang et al., 2025; Kamali Dolatabadi et al., 2023).

Table 1. Silica (SiO_2) content in raw and acid-washed fly ash, and pure silica as reference

Sample	SiO_2 content (mg/kg)
Fly ash (FA)	32.867
FA after HCl washing	46.016
Pure silica (SiO_2)	71.053

FTIR spectra and validation of silica functionalization

The FTIR spectrum of the ethylenediamine-functionalized silica xerogel (SiO_2@EDA) is presented in Figure 1, providing crucial insights into the functional groups and framework integrity. Correlating with Table 1, the increase in the SiO_2 content after acid treatment supports the successful removal of metal oxides and enhancement of the silica network, which is further corroborated by the FTIR data. Similar observations were reported by Badr et al., (2025) and Tran et al., (2025), where acid purification led to increased Si–O–Si signal intensity, reflecting a more developed silica framework (Alatawi, 2025; Badr et al., 2025; Sarkar and Mondal, 2024)

A strong absorption band in the 1000–1400 cm^{-1} region, with a peak at ~1055 cm^{-1} and a shoulder between 980–1350 cm^{-1}, corresponds to asymmetric stretching vibrations of siloxane bridges (Si–O–Si) – the fundamental structural motif of three-dimensional silica networks (Alatawi, 2025; Badr et al., 2025; Sarkar and Mondal, 2024). Additional peaks at 776 cm^{-1} and ~450 cm^{-1} are attributed to symmetric vibrations and bending of silanol (Si–OH) groups, suggesting the presence of free hydroxyls in the amorphous silica matrix (Guesmi et al., 2025; Obaid et al., 2025; Shi et al., 2025). These features are consistent with the results reported by Marhoon et al., (2024), who demonstrated the functional role of silanol groups in facilitating chemical modifications on the xerogel surfaces derived from industrial waste.

A broad O–H band near 3530 cm^{-1} and a bending vibration at 1645 cm^{-1} indicate adsorbed or hydrogen-bonded water. However, the band at 1645 cm^{-1} may also obscure the characteristic deformation of NH_2 groups, complicating spectral interpretation (Al-Wabsi and Alshareef, 2025; Marhoon et al., 2024; Pandey et al., 2025; Tran et al., 2025). Tan et al., (2021) similarly highlighted that spectral overlap between O–H and NH_2 bands often hinders clear identification of amine functionalities in modified silica systems. Vibrations of C–N bonds (1000–1250 cm^{-1}) from aliphatic amines are also masked by the dominant Si–O–Si framework bands. Nonetheless, the CH_2 stretching vibrations from ethylenediamine are evident in the 2840–2980 cm^{-1} region (Al-Wabsi and Alshareef, 2025;

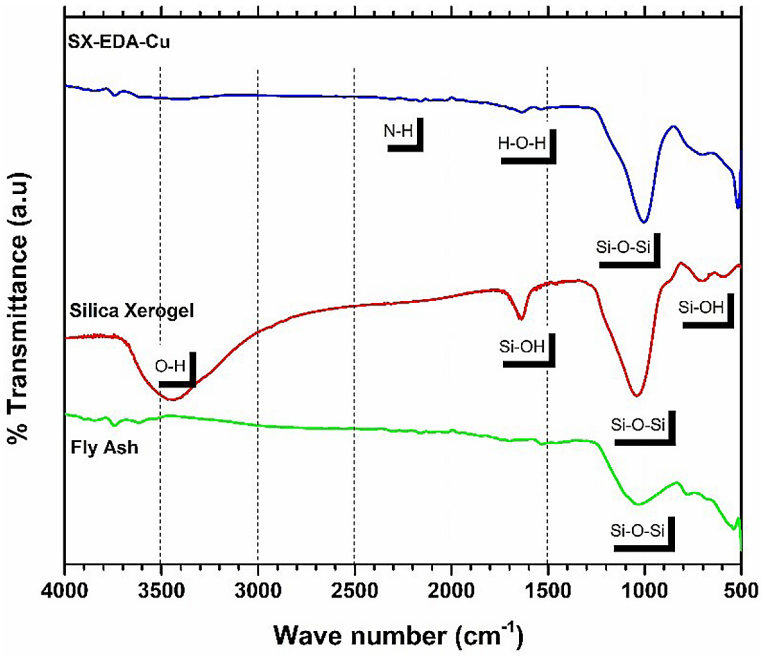

Figure 1. FTIR spectrum of fly ash, silica xerogel and modified silica xerogel

Pandey et al., 2025), serving as indirect indicators of successful ethylenediamine incorporation. Naushad et al., (2019) and Wang et al., (2019) also emphasized that CH_2 peaks can validate the covalent integration of amine groups into silica matrices.

The results of this study lies in employing ethylenediamine as a surface functionalizing agent for the xerogel silica derived from purified fly ash. Unlike conventional post-synthesis adsorption techniques, the co-condensation approach during the sol–gel process yields a homogeneous silica network with covalently embedded $–NH_2$ groups. This results in improved chemical stability and specific interaction capabilities, as confirmed by the FTIR data and increased SiO_2 content in Table 1. These findings are consistent with the work of Alqadami et al., (2020), who underscored the importance of amine incorporation into silica frameworks for enhanced stability and adsorption performance toward heavy metal ions and organic pollutants.

Crystal structure and purification efficiency based on the XRD analysis

The X-ray diffraction patterns presented in Figure 2 illustrate the significant structural transformation of the materials from raw fly ash (FA) to synthesized silica xerogel (SiO_2) and finally to the modified silica (SiO_2@EDA–Cu). In the case of FA, sharp diffraction peaks are observed around $2\theta = 26.5°$ and 33.2°, corresponding to quartz (SiO_2) and hematite (Fe_2O_3), respectively. These peaks indicate the presence of crystalline phases typical of coal combustion residues (Hammad et al., 2025; Rahman et al., 2025; Zheng et al., 2025). The presence of Fe_2O_3 suggests that the initial purification step did not fully eliminate metallic impurities. This finding aligns with Hayati et al., (2017), who reported residual quartz and hematite as common crystalline contaminants in raw FA prior to leaching.

In contrast, the XRD patterns of the silica xerogel and modified materials exhibit a broad, low-intensity hump in the range of $2\theta = 21–23°$, which is characteristic of amorphous silica. This amorphous structure is highly desirable for applications in adsorption and catalysis due to its high surface area and porous morphology (Al-Hazmi et al., 2025). Similar amorphous features were also reported by Hannachi et al. (2019) and Hu et al. (2022), who observed that the silica xerogels synthesized from inorganic waste via sol–gel processes tend to form disordered networks due to incomplete hydrolysis and condensation reactions.

Interestingly, no distinct peaks corresponding to NaCl, CaO, or other alkali-containing compounds were detected in the XRD patterns of either silica product. This indicates that the acid-washing step using HCl was effective in removing interfering ions – especially sodium and calcium – which are known to block pores and

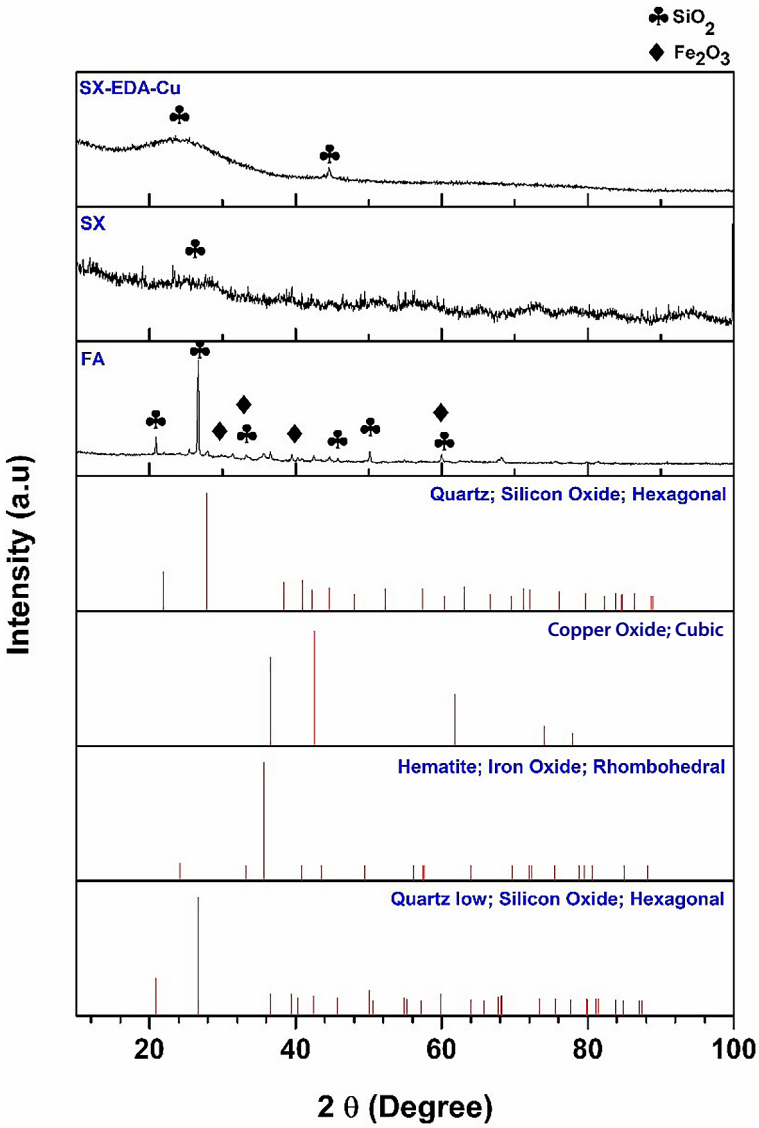

Figure 2. XRD diffraction of each material

destabilize xerogel structures (Akti and Balci, 2023; Souto and Machado, 2023; Zheng et al., 2024). This outcome is consistent with the findings from Zhou et al. (2024), who emphasized that the presence of alkali metal cations can negatively affect the structural stability and adsorption capacity of the FA-derived xerogels.

This conclusion is further supported by the increasing SiO_2 content in Table 1 – from 32.867% in FA to 46.016% after acid washing, and finally to 71.053% in the final product – demonstrating the effectiveness of both the purification and synthesis steps in enhancing the structural as well as chemical quality of the material. These results are in agreement with studies by Hannachi et al., (2019) and Hasanpour and Hatami, (2020), who showed that acid leaching significantly improves silica purity and reduces heavy metal content in FA. When combined with sol–gel synthesis, the process yields an amorphous, structurally stable, and surface-reactive silica material.

The results of this study liein its integrative strategy, which combines acid leaching, sol–gel synthesis, and chemical surface modification with EDA and $CuCl_2$. This approach not only enhances the purity and amorphous nature of the resulting silica but also introduces functional surface groups that improve selective adsorption performance toward heavy metal ions. The studies combining both amine functionalization and metal ion impregnation in FA-based xerogel systems remain scarce, making this work a valuable scientific contribution to the development of functional adsorbents derived from industrial solid waste.

In conclusion, the integration of XRD results with the oxide composition data in Table 1

confirms that the purification and synthesis strategy employed in this study effectively transformed raw fly ash into high-quality amorphous silica. The final material is free from residual crystalline impurities and structurally suited for advanced functional applications, particularly in the adsorption of heavy metals from aqueous environments.

Pore texture characterization based on BET adsorption and BJH pore distribution

The nitrogen adsorption–desorption isotherms of fly ash, silica xerogel (SiO_2), and the functionalized silica (SiO_2@NH_2–Cu) are shown in Figure 3, while the estimated pore textural properties of each material are summarized in Table 2. According to IUPAC classification, the silica xerogel exhibits a Type IV isotherm with an H3 hysteresis loop, indicating the presence of both mesoporous and microporous structures – an ideal feature for liquid-phase adsorption applications (Kaya et al., 2021; Pilato et al., 2025; Souto and Machado, 2023). The pore diameter distribution derived from the BJH analysis shows a gradual increase from 1.78 nm (fly ash), to 2.504 nm (SiO_2 xerogel), and finally to 16.089 nm (SiO_2@NH_2–Cu), reflecting the structural evolution from raw material to a chemically modified mesoporous adsorbent.

The transformation of fly ash into silica xerogel led to a substantial increase in specific surface area from 6.025 m²/g to 134.392 m²/g, which corresponds well with the enhancement in SiO_2 purity from 32.867% to 71.053%, as shown in Table 1. This confirms the effectiveness of the silica extraction and purification process. Further surface modification using ethylenediamine and Cu^{2+} ions resulted in a moderate decrease in surface area to 77.415 m²/g, a phenomenon commonly attributed to partial pore blocking by amine groups and Cu species on the silica framework (Taleb et al., 2024). However, the pore volume increased significantly from 0.1184 to 0.3894 cm³/g, along with a marked enlargement in pore diameter to 16.089 nm. This increase in porosity is likely due to the strong interaction between EDA and the silica walls during the sol–gel process, which alters the local pH and promotes the formation of larger pores (Gong et al., 2025).

To strengthen the discussion, the textural properties of the synthesized SiO_2@NH_2–Cu adsorbent were compared with of similar functionalized silica-based materials reported in the literature. Table 3 summarizes the BET surface area, pore diameter, pore volume, and functional characteristics of selected adsorbents.

Although some amine-functionalized silica materials reported surface areas ranging from 150–800 m²/g, many exhibited pore diameters below 6 nm (Ezzeddine et al., 2025; Vareda et al., 2020). In contrast, the SiO_2@NH_2–Cu produced in this work demonstrates a significantly larger pore diameter (16.089 nm), which is advantageous for the adsorption of larger ionic species and hydrated metal complexes. Additionally, the dual functionalization – introduction of $–NH_2$ groups and coordination of Cu^{2+} – creates synergistic active sites that are absent in most conventional mesoporous silica materials.

This comparison highlights that although the surface area of SiO_2@NH_2–Cu is moderate, its expanded mesopore structure and multifunctional surface chemistry provide superior potential for heavy metal adsorption relative to similar materials.

Table 2. Textural properties of materials based on BET and BJH analysis

Material	Surface area (m²/g)	Pore volume (cm³/g)	Pore diameter (nm)
Fly ash (FA)	6.025	0.0136	1.78
Silica xerogel	134.392	0.1184	2.5
SiO_2@NH_2–Cu	77.415	0.3894	16.09

Table 3. Comparison of textural parameters with literature reports

Material	Surface area (m²/g)	Pore diameter (nm)	Functional groups	Reference
Amine-silica	150–300	3–6	$–NH_2$	Vareda et al., 2020
Cu-loaded silica	90–150	4–8	Cu–O	Ezzeddine et al., 2025
Fly ash silica xerogel	134.392	2.504	Si–OH	This study
SiO_2@NH_2–Cu	77.415	16.089	$–NH_2$ + Cu^{2+}	This study

A similar reduction in surface area following functionalization was reported by Ávila et al., (2025), where the introduction of organic moieties or metal ions frequently led to partial obstruction of the pore network. Nevertheless, the significant increases in pore volume and diameter offer a functional advantage for adsorption applications, particularly in the capture of heavy metal ions, such as Cu^{2+}, Pb^{2+}, and Cr^{3+}.

The novelty of this study lies in three main aspects. First, the use of locally sourced fly ash as a precursor for mesoporous silica represents a circular economy approach to valorizing industrial waste, which remains underexplored in the context of functional adsorbent development. Second, the in situ chemical modification using ethylenediamine and Cu^{2+} enables the formation of a structurally open and surface-functionalized silica adsorbent with tunable properties. Third, the synergistic integration of silica purity improvement (Table 1) and pore textural optimization (Table 2) demonstrates that the synthesized hybrid material holds significant promise as a renewable adsorbent for environmental remediation, especially in tackling heavy metal contamination in wastewater systems.

Figure 3 illustrates the nitrogen adsorption–desorption isotherms (top row) and the corresponding pore size distribution curves (bottom row) for fly ash, silica xerogel, and modified silica xerogel (SiO_2@NH_2–Cu). All materials exhibit Type IV isotherms with H3-type hysteresis loops, which are characteristic of mesoporous materials with slit-shaped pores formed by the aggregation of plate-like particles (Thommes et al., 2015). The occurrence of hysteresis in the relative pressure range of $p/p_0 = 0.4–1.0$ indicates capillary condensation within mesopores, affirming their mesostructural nature.

The fly ash sample exhibits a relatively low nitrogen uptake, with a narrow hysteresis loop and a broad, poorly defined pore size distribution centered around 11.7 nm. This suggests the presence of heterogeneous mesopores with limited specific surface area and poorly connected pore networks. Similar features have been reported in untreated fly ash materials, which typically exhibit irregular porosity due to the variability of their mineral constituents (Wang et al., 2021).

In contrast, the silica xerogel sample shows a substantially higher volume of adsorbed nitrogen, with a pronounced hysteresis loop and a sharp desorption branch. This behavior is indicative of a well-developed mesoporous framework with higher pore volume and surface area. The dominant pore size at approximately 4.76 nm suggests the presence of uniform mesopores formed through sol–gel processing under controlled hydrolysis–condensation conditions (Yücel et al., 2016). These characteristics are typical

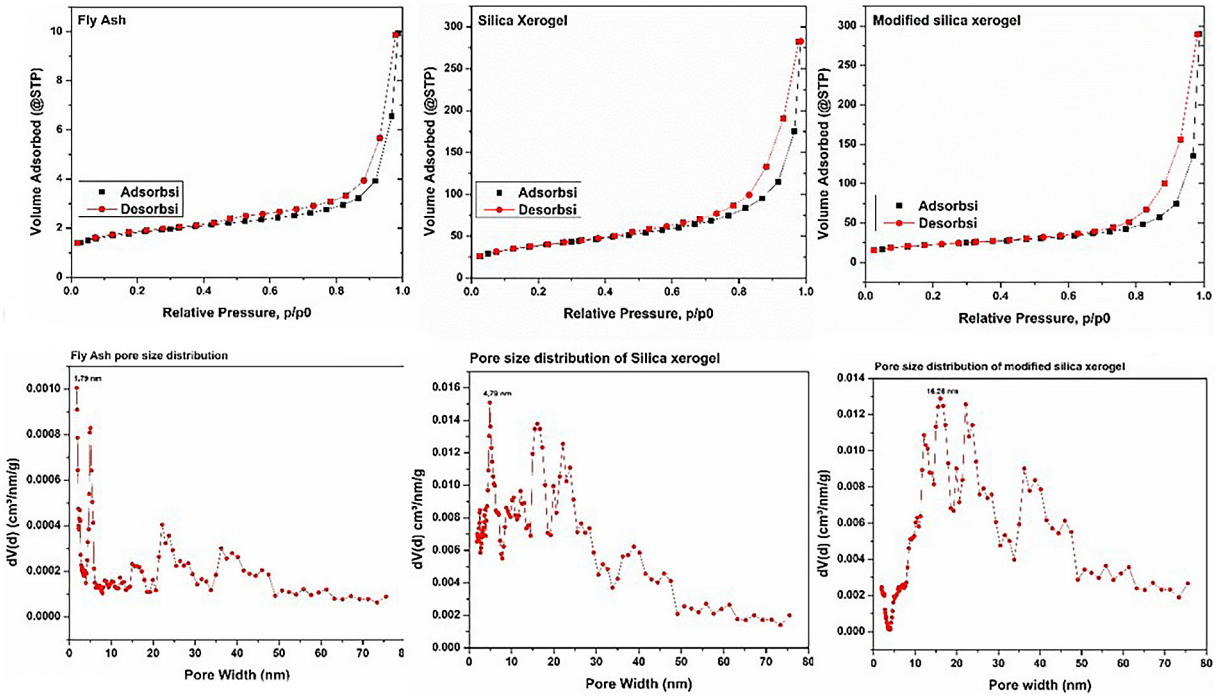

Figure 3. N_2 adsorption-desorption and pore size distribution of each material

of classical silica xerogels synthesized in acidic media and dried under ambient conditions.

For the modified silica xerogel (SiO_2@NH_2–Cu), a comparable isotherm shape is observed, but the total adsorbed volume is slightly reduced, likely due to partial pore blockage by surface-grafted ethylenediamine and Cu^{2+} species. Notably, the pore size distribution shifts toward larger mesopores, with a peak around 10.48 nm. This increase may be attributed to structural rearrangements during functionalization, potentially caused by interactions between amine groups and the siloxane network or by localized swelling of the matrix (Soroceanu and Stiubianu, 2021).

Consistent findings have been reported by Bae et al. (2025), who observed a reduction in BET surface area and pore volume following amine functionalization, without compromising mesopore integrity. The introduction of amine groups enhances the surface chemical affinity for metal ions by providing additional coordination sites. Ezzeddine et al. (2025) further reported that functionalized silica materials often exhibit broadened pore size distributions and wider hysteresis loops, attributed to increased pore interconnectivity and structural flexibility. Thommes et al. (2015) emphasized that while surface area may decline upon functionalization, adsorption capacity and selectivity toward heavy metals are significantly enhanced due to the availability of functional moieties, such as $–NH_2$ and immobilized metal ions like Cu^{2+}.

Overall, the data confirm that functionalization of silica xerogel with ethylenediamine and $CuCl_2$ successfully introduces chemical functionality without severely disrupting the mesoporous architecture. This dual benefit – preserved porosity and enhanced surface reactivity – makes the modified xerogel a promising candidate for use in adsorption-based removal of contaminants or in the catalytic systems requiring accessible active sites (Bailón-García et al., 2020; Vareda et al., 2020).

Surface morphology and elemental composition (FESEM–EDS analysis)

The surface morphology of the synthesized materials was investigated using FESEM, as presented in Figure 4. Raw fly ash exhibited an irregular, porous, and agglomerated structure (Figure 4a), which is consistent with previous studies indicating the presence of amorphous aluminosilicates and heterogeneous mineral particles in coal-derived fly ash (Shoppert et al., 2020). Such surface features provide abundant active sites for further chemical modification and potential applications in adsorption processes.

In contrast, the Si@NH_2 material (Figure 4b) showed significant morphological transformation with the appearance of finer, more uniformly distributed spherical particles. The observed increase in roughness and surface area suggests successful grafting of ethylenediamine groups, which disrupts the original particle agglomeration and enhances homogeneity. This morphological improvement aligns with the findings by Chen et al., (2022), who demonstrated that amine-functionalization of silica introduces hydrophilic groups and increases colloidal stability—beneficial for dispersion in aqueous environments and metal ion capture.

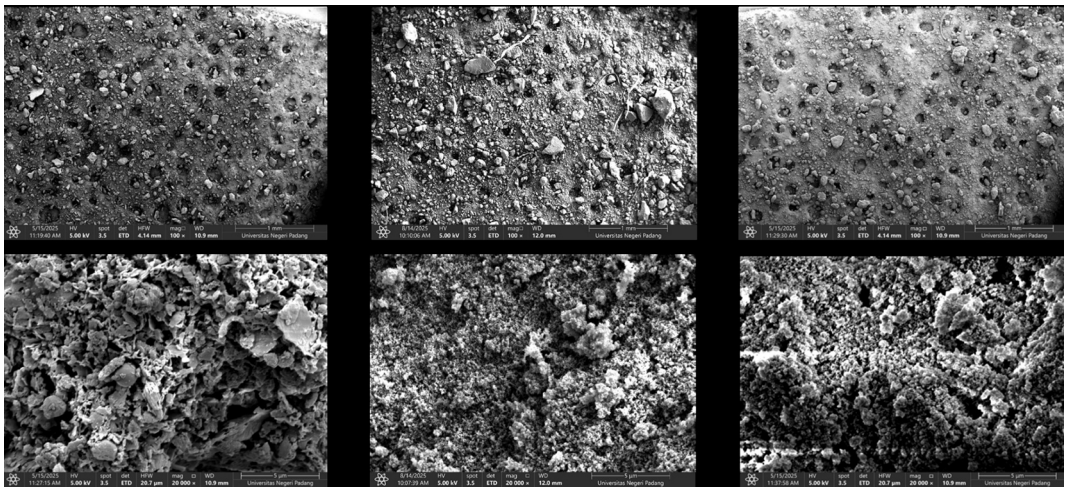

Figure 4. Surface morphology from FESEM characterization for: a) fly ash, b) SiO_2, and c) SiO_2@NH_2-Cu

Following Cu^{2+} impregnation (Figure 4c), the surface of Si@NH_2–Cu retained the roughened structure but appeared denser, indicating the coordination of Cu^{2+} ions onto the amine-modified silica framework. The uniform coverage of Cu across the particle surface implies that both the EDA and Cu precursors were successfully anchored during the sol–gel synthesis. Similar morphologies have been reported in the Cu-loaded mesoporous silica xerogels and hybrid nanocomposites used for catalysis and adsorption (Chen et al., 2022; Gencer Balkis et al., 2025).

Elemental composition was further analyzed using energy dispersive x-ray spectroscopy (EDS), as shown in Figure 5. The EDS spectrum of raw fly ash (Figure 5a) revealed a high abundance of oxygen (48.10 wt%), silicon (19.56 wt%), aluminum (11.22 wt%), and calcium (7.74 wt%), along with minor fractions of iron and magnesium. These results confirm the presence of aluminosilicate structures, which are typical of fly ash produced from coal combustion (Balkis et al., 2025). The presence of calcium and iron oxides further contributes to the surface reactivity and adsorptive potential of the material.

After surface modification, the EDS profile of Si@NH_2–Cu (Figure 5b) displayed new peaks corresponding to nitrogen (1.45 wt%), carbon (16.70 wt%), and copper (0.46 wt%). The carbon and nitrogen signals confirm the successful grafting of ethylenediamine moieties, while the copper peaks at ~0.9 keV and ~8.0 keV (Cu Lα and Cu Kα) indicate the effective incorporation of Cu^{2+} ions. These findings are consistent with those reported by Y. Chen et al., (2022), who noted similar elemental signatures in the Cu-chelated amine-functionalized silica. The persistent presence of silicon and oxygen underscores the structural stability of the silica framework during modification. A minor gold (Au) signal, originating from sputter coating for FESEM analysis, was also detected. Traces of Na and Al may derive from residual fly ash components, which were not fully removed during purification.

These observations were further corroborated by FTIR analysis, which detected –NH_2 stretching and bending vibrations near 3300 and 1550 cm^{-1}, respectively, providing chemical evidence of successful amine functionalization. It was emphasized that nitrogen and carbon peaks are reliable markers of organic modification on silica-based surfaces (Yan et al., 2023). Moreover, the detection of Cu^{2+} on the modified surface is critical, as it introduces new active sites capable of participating in ion exchange and coordination reactions essential for heavy metal adsorption.

Compared to previous studies, this work introduced a novel combination of sol–gel synthesis using fly ash, EDA functionalization, and Cu^{2+} impregnation in a single platform. Most existing literature utilizes commercial silica or untreated ash without sequential modification (Aigbe et al., 2021; Ijaz et al., 2025). Here, the integration of industrial by-products into value-added adsorbents exemplifies a sustainable strategy in line with green chemistry principles. Furthermore, the convergence of the FESEM–EDS data with elemental content in Table 1 confirms the transformation of the silica structure both morphologically and chemically into a material with promising adsorptive capabilities.

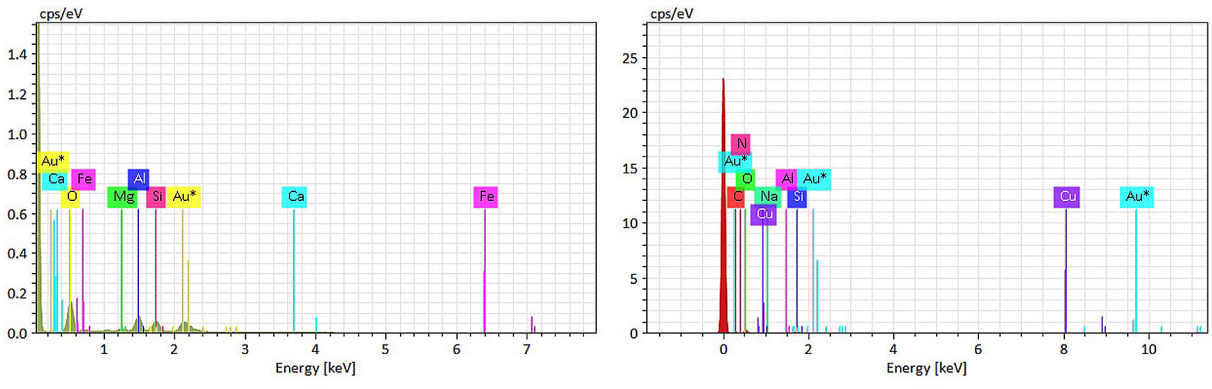

Figure 5. Elemental content contained in (a) fly ash, and (b) Si@NH_2-Cu material from EDS measurment

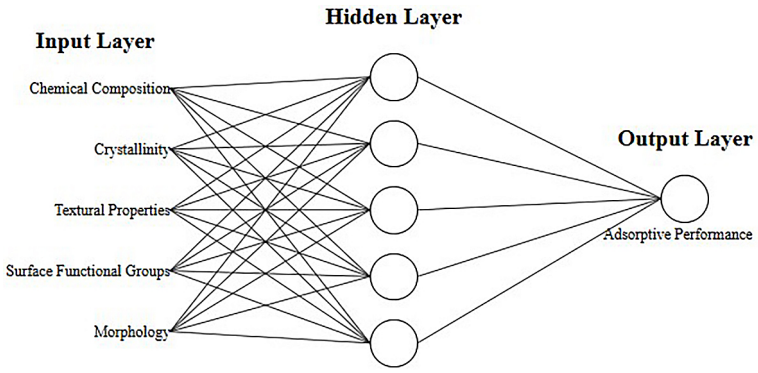

Figure 6. Artificial neural network modeling

Artificial neural network modeling for adsorption performance prediction

To better understand and predict the adsorption performance of ethylenediamine–Cu^{2+} functionalized silica xerogel (SiO_2@NH_2–Cu), an ANN model was developed. ANN has been widely employed in environmental and materials engineering to model complex, nonlinear relationships between material properties and functional performance (Fiyadh et al., 2023; Narayana et al., 2021). In this study, the ANN model utilized structural, textural, chemical, and surface functionalization data as input parameters to predict heavy metal adsorption efficiency (Figure 6).

The characterization of the functionalized silica xerogel was conducted using multiple complementary techniques. Elemental composition, including SiO_2, N, Cu, O, Al, and Ca, was determined via elemental analysis and energy dispersive spectroscopy. Crystallinity and structural properties were evaluated using X-ray diffraction, providing insight into the degree of amorphousness. Textural properties, such as specific surface area, pore volume, and average pore diameter, were assessed using BET and BJH analyses. Surface functional groups, including $–NH_2$ and $–CH_2–$ moieties, were confirmed through FTIR spectroscopy, indicating successful chemical modification. Morphological features, such as particle size distribution and surface roughness, were examined using FESEM, revealing detailed information on the topography and surface structure of the xerogel.

The ANN architecture consisted of an input layer corresponding to the features above, two hidden layers to capture nonlinear interactions among pore structure, surface chemistry, and Cu^{2+} incorporation, as well as an output layer representing the predicted adsorption capacity (mg/g) or removal efficiency (%). The hidden layers employed ReLU activation functions, while the output layer used a linear activation function to allow continuous prediction. The model was trained using backpropagation with the Adam optimizer, minimizing the mean squared error between predicted and experimental adsorption values.

The ANN model effectively captured the complex dependencies of adsorption efficiency on physicochemical properties. Sensitivity analysis revealed that pore size distribution, $–NH_2$ functional group density, and Cu^{2+} content were the most influential parameters, consistent with previous studies highlighting the critical role of mesoporosity and surface functionalities in enhancing metal ion adsorption (Fiyadh et al., 2023; Kumari et al., 2022).

Overall, the ANN modeling demonstrates a powerful predictive tool for designing functionalized silica adsorbents and optimizing synthesis parameters for enhanced environmental remediation applications.

It is important to note that the present study focused primarily on the synthesis and comprehensive characterization of SiO_2@NH_2–Cu. The adsorption application phase has not been initiated yet; therefore, experimental adsorption capacities, isotherms, or kinetic results are not included in this manuscript. The ANN model was employed as a predictive tool to explore the relationship between structural parameters and potential adsorption behavior, serving as a foundation for future work in which adsorption experiments will be conducted and reported.

CONCLUSIONS

This study highlighted the transformation of fly ash into a functionalized silica xerogel (SiO_2@ NH_2–Cu) through acid leaching, sol–gel synthesis, and surface modification with ethylenediamine and Cu^{2+}. Acid treatment effectively increased the SiO_2 content, removing impurities and enhancing precursor reactivity, while XRD confirmed amorphous silica formation suitable for adsorption. Nitrogen adsorption–desorption (BET/BJH) revealed a mesoporous network with enlarged pore diameter and high pore volume despite moderate surface area reduction due to functionalization. The FESEM–EDS analysis demonstrated uniform particle morphology with successful grafting of amine groups and Cu^{2+} incorporation. An ANN model further predicted adsorption efficiency, identifying pore architecture, $–NH_2$ density, and Cu content as primary factors. Overall, SiO_2@NH_2–Cu exhibits enhanced surface chemistry, stable mesoporosity, and promising heavy metal adsorption capacity, supporting its potential as a renewable adsorbent for environmental remediation.

Acknowledgments

The authors express their gratitute to LPPM Universitas Andalas for providing financial via "Penelitian Disertasi Doktor Batch 1" No. 82/ UN16.19/PT.01.03/PDD/2025.

REFERENCES

1. Abidli, A., Ben Rejeb, Z., Zaoui, A., Naguib, H. E., Park, C. B. (2025). Comprehensive insights into the application of graphene-based aerogels for metals removal from aqueous media: Surface chemistry, mechanisms, and key features. *Advances in Colloid and Interface Science*, *335*. https://doi.org/10.1016/j.cis.2024.103338
2. Aigbe, U. O., Ukhurebor, K. E., Onyancha, R. B., Osibote, O. A., Darmokoesoemo, H., Kusuma, H. S. (2021). Fly ash-based adsorbent for adsorption of heavy metals and dyes from aqueous solution: A review. *Journal of Materials Research and Technology*, *14*, 2751–2774. https://doi.org/10.1016/j.jmrt.2021.07.140
3. Akti, F., Balci, S. (2023). Silica xerogel and iron doped silica xerogel synthesis in presence of drying control chemical additives. *Materials Chemistry and Physics*, *297*, 127347. https://doi.org/10.1016/j.matchemphys.2023.127347
4. Al-Hazmi, G. H., Albedair, L. A., Alsuhaibani, A. M., Alrefaee, S. H., Althagafi, I., Mohsen, Q., El-Desouky, M. G., El-Bindary, A. A., Asla, K. A. (2025). Synthesis and characterization of functionalized yttrium metal-organic frameworks encapsulated onto bi-polymers for effective removal of As(III); Adsorption isotherms, kinetic, and optimization via Box-Behnken design. *Materials Today Communications*, *45*, 112244. https://doi.org/10.1016/j.mtcomm.2025.112244
5. Al-Wabsi, M. S., Alshareef, S. A. (2025). Elimination of industrial dye from wastewater through alginate/polyethylenimine hydrogel beads infused with selenium metal-organic framework: Evaluating adsorption isotherms, kinetics, and optimization techniques. *Materials Today Communications*, *47*, 113042. https://doi.org/10.1016/j.mtcomm.2025.113042
6. Alatawi, R. A. S. (2025). Electrospun nanofiber chitosan/polyvinyl alcohol loaded with metal organic framework nanofiber for efficient adsorption and removal of industrial dyes from waste water: Adsorption isotherm, kinetic, thermodynamic, and optimization via Box-Behnken design. *International Journal of Biological Macromolecules*, *299*, 140086. https://doi.org/10.1016/j.ijbiomac.2025.140086
7. Alqadami, A. A., Naushad, M., Ahamad, T., Algamdi, M., Alshahrani, A., Uslu, H., Shukla, S. K. (2020). Removal of highly toxic cd(Ii) metal ions from aqueous medium using magnetic nanocomposite: Adsorption kinetics, isotherm and thermodynamics. *Desalination and Water Treatment*, *181*, 355–361. https://doi.org/10.5004/dwt.2020.25108
8. Ávila, F. G., Cabrera-Sumba, J., Valdez-Pilataxi, S., Villalta-Chungata, J., Valdiviezo-Gonzales, L., Alegria-Arnedo, C. (2025). Removal of heavy metals in industrial wastewater using adsorption technology: Efficiency and influencing factors. *Cleaner Engineering and Technology*, *24*. https://doi.org/10.1016/j.clet.2025.100879
9. Badr, M. M., Selim, M. S., Youssef, W. M. (2025). Synthesis of silicone material organo-cured with thiourea and methyl methacrylate for heavy metals adsorption from polluted water. *Inorganic Chemistry Communications*, *172*, 113714. https://doi.org/10.1016/j.inoche.2024.113714
10. Bae, J. Y., Jang, S. G., Cho, J., Kang, M. (2025). Amine-functionalized mesoporous silica for efficient CO_2 capture: Stability, performance, and industrial feasibility. *International Journal of Molecular Sciences 26*(9). https://doi.org/10.3390/ijms26094313
11. Bailón-García, E., Drwal, E., Grzybek, T., Henriques, C., Ribeiro, M. F. (2020). Catalysts based on carbon xerogels with high catalytic activity for the reduction of NOx at low temperatures. *Catalysis Today*, *356*, 301–311. https://doi.org/https://doi.org/10.1016/j.cattod.2020.03.004
12. Chang, C., Tao, S., Xu, C., Zhang, Y., Jiang, W., Cao, Y., Ma, C. (2025). Highly transparent polymethylsilsesquioxane xerogel monoliths with nanopores around 10 nm via ambient pressure drying: A potential host for nano-functional materials.

Journal of Luminescence, *286*, 121353. https://doi.org/10.1016/j.jlumin.2025.121353

13. Chen, Y., Jia, S., Zhao, W., Song, J., Li, Y., Wang, H. (2022). Ethylenediamine functionalized chelating resin for removal of Cu(II) and Cd(II) from aqueous solution. *Desalination and Water Treatment*, *274*, 206–218. https://doi.org/10.5004/dwt.2022.28915
14. Da'na, E. (2017). Adsorption of heavy metals on functionalized-mesoporous silica: A review. *Microporous and Mesoporous Materials*, *247*, 145–157. https://doi.org/10.1016/j.micromeso.2017.03.050
15. Das, P. N., Jithesh, K., Raj, K. G. (2021). Recent developments in the adsorptive removal of heavy metal ions using metal-organic frameworks and graphene-based adsorbents. *Journal of the Indian Chemical Society*, *98*(11), 100188. https://doi.org/10.1016/j.jics.2021.100188
16. de Souza, M., Frias, J. P. G. L., Nash, R., He, D., Luo, Y., Lu, S., Liu, M., Song, Y., Lei, L., Abel, A., Machado, D. S., Kloas, W., Zarfl, C., Rillig, M. C., Novotna, K., Cermakova, L., Pivokonska, L., Cajthaml, T., Pivokonsky, M.,… Nash, R. (2019). Microplastics in drinking water treatment – current knowledge and research needs. *Science of the Total Environment*, *111*, 37–46. https://doi.org/10.1111/gcb.14020.Microplastics
17. Eteba, A., Bassyouni, M., Saleh, M. (2023). Utilization of chemically modified coal fly ash as cost-effective adsorbent for removal of hazardous organic wastes. *International Journal of Environmental Science and Technology*, *20*(7), 7589–7602. https://doi.org/10.1007/s13762-022-04457-5
18. Ezzeddine, Z., Batonneau-Gener, I., Ghssein, G., Pouilloux, Y. (2025). Recent Advances in heavy metal adsorption via organically modified mesoporous silica: A review. *Water (Switzerland)*, *17*(5), 1–17. https://doi.org/10.3390/w17050669
19. Fan, Y., Feng, K., Xie, P., Tian, H., Wu, Y., Zhou, F. (2025). Recyclable cellulose nanocrystals xerogel with thermally insulating and radiative cooling. *Sustainable Materials and Technologies*, *43*, e01334. https://doi.org/10.1016/j.susmat.2025.e01334
20. Fernandes, J., Fernandes, A. C., Echeverría, J. C., Moriones, P., Garrido, J. J., Pires, J. (2019). Adsorption of gases and vapours in silica based xerogels. *Colloids and Surfaces A: Physicochemical and Engineering Aspects*, *561*, 128–135. https://doi.org/10.1016/j.colsurfa.2018.10.063
21. Fiyadh, S. S., Alardhi, S. M., Al Omar, M., Aljumaily, M. M., Al Saadi, M. A., Fayaed, S. S., Ahmed, S. N., Salman, A. D., Abdalsalm, A. H., Jabbar, N. M., El-Shafi, A. (2023). A comprehensive review on modelling the adsorption process for heavy metal removal from waste water using artificial neural network technique. *Heliyon*, *9*(4), e15455. https://doi.org/10.1016/j.heliyon.2023.e15455
22. Gaur, N., Kukreja, A., Yadav, M., Tiwari, A. (2018). Adsorptive removal of lead and arsenic from aqueous solution using soya bean as a novel biosorbent: equilibrium isotherm and thermal stability studies. *Applied Water Science*, *8*(4), 1–12. https://doi.org/10.1007/s13201-018-0743-5
23. Gencer Balkis, B., Aksu, A., Ersoy Korkmaz, N., Taskin, O. S., Celen, C., Caglar Balkis, N. (2025). Synthesis of silica-chitosan nanocomposite for the removal of pharmaceuticals from the aqueous solution. *International Journal of Environmental Science and Technology*, *22*(1), 153–168. https://doi.org/10.1007/s13762-024-05919-8
24. Gong, D., Li, J., Wang, Z., Zha, X., Zhang, C. (2025). A "Two birds one Stone" strategy for preparing chemically modified phenolic xerogels with inner pore surfaces for heavy metal ion adsorption. *Separation and Purification Technology*, *365*, 132621. https://doi.org/10.1016/j.seppur.2025.132621
25. Guesmi, A., Hamadi, N. Ben, El-Fattah, W. A., Subaihi, A., Alluhaybi, A. A., El-Desouky, M. G., El-Bindary, A. A. (2025). Efficient removal of Pb(II) ions from wastewater via a vanadium metal-organic framework encapsulated with biopolymer carboxymethyl cellulose/polyethylenimine through synthesis, characterization, and Box-Behnken optimization. *International Journal of Biological Macromolecules*, *318*(P3), 145201. https://doi.org/10.1016/j.ijbiomac.2025.145201
26. Guzel Kaya, G., Aznar, E., Deveci, H., Martínez-Máñez, R. (2021). Low-cost silica xerogels as potential adsorbents for ciprofloxacin removal. *Sustainable Chemistry and Pharmacy*, *22*. https://doi.org/10.1016/j.scp.2021.100483
27. Hammad, W. A., Alqahtani, F. M., Darweesh, M. A., Amr, M. H. A., Eweida, B., Bakr, A. (2025). Innovative methods using palm frond-derived activated carbon for Cu (II) adsorption. *Materials Chemistry and Physics*, *339*. https://doi.org/10.1016/j.matchemphys.2025.130568
28. Hannachi, Y., Hafidh, A., Ayed, S. (2019). Effectiveness of novel xerogels adsorbents for cadmium uptake from aqueous solution in batch and column modes: Synthesis, characterization, equilibrium, and mechanism analysis. *Chemical Engineering Research and Design*, *143*, 11–23. https://doi.org/10.1016/j.cherd.2019.01.006
29. Hasanpour, M., Hatami, M. (2020). Application of three dimensional porous aerogels as adsorbent for removal of heavy metal ions from water/wastewater: A review study. *Advances in Colloid and Interface Science*, *284*, 102247. https://doi.org/10.1016/j.cis.2020.102247
30. Hayati, B., Maleki, A., Najafi, F., Daraei, H., Gharibi, F., McKay, G. (2017). Adsorption of Pb^{2+}, Ni^{2+}, Cu^{2+}, Co^{2+} metal ions from aqueous solution by PPI/SiO2 as new high performance adsorbent: Preparation, characterization, isotherm, kinetic, thermodynamic studies. *Journal of Molecular Liquids*, *237*, 428–436. https://doi.org/10.1016/j.molliq.2017.04.117
31. Hu, T. T., Liu, F., Dou, S., Zhong, L. Bin, Cheng, X., Shao, Z. D., Zheng, Y. M. (2022). Selective adsorption of trace gaseous ammonia from air by a sulfonic acid-modified silica xerogel: Preparation, characterization

and performance. *Chemical Engineering Journal*, *443*, 136357. https://doi.org/10.1016/j.cej.2022.136357

32. Ijaz, A., Sahin, K., Dirak, M., Yagci, M. B., Kolemen, S., Demirel, A. L., Miko, A. (2025). Development of novel iron and copper-loaded mesoporous silica particles with exceptional visible-light-induced photocatalytic properties for ultra-fast removal of organic pollutants from wastewater. *Journal of Water Process Engineering*, *75*, 108050. https://doi.org/10.1016/j.jwpe.2025.108050
33. Kamali Dolatabadi, A., Mokhtari, J., Talebian, N. (2023). Silica xerogel carrier as encapsulating Material for the in-vitro controlled release of montelukast. *Inorganic Chemistry Communications*, *149*, 110378. https://doi.org/10.1016/j.inoche.2022.110378
34. Kumari, A., Rajput, V. D., Mandzhieva, S. S., Rajput, S., Minkina, T., Kaur, R., Sushkova, S., Kumari, P., Ranjan, A., Kalinitchenko, V. P., Glinushkin, A. P. (2022). Microplastic pollution: An emerging threat to terrestrial plants and insights into its remediation strategies. *Plants*, *11*(3), 1–14. https://doi.org/10.3390/plants11030340
35. Lewińska, I., Bącal, P., Tymecki, Ł. (2024). Hydrogen peroxide stabilization with silica xerogel for paper-based analytical devices and its application to phenolic compounds determination. *Analytica Chimica Acta*, *1320*. https://doi.org/10.1016/j.aca.2024.343028
36. Li, C., Wang, Y. (2025). Iron/silicon oxy-hydroxide co-precipitate trace-incorporated [-Fe-O]m-[Si-O-]n colloids: A facile strategy for silica xerogel strengthening and toughening. *Construction and Building Materials*, *461*. https://doi.org/10.1016/j.conbuildmat.2025.139895
37. Mahdi, A. H., Jaid, G. M., Alardhi, S. M. (2021). Artificial neural network modelling for the removal of lead from wastewater by using adsorption process. *Desalination and Water Treatment*, *244*, 110–119. https://doi.org/10.5004/dwt.2021.27914
38. Marhoon, A. A., Hasbullah, S. A., Asikin-Mijan, N., Mokhtar, W. N. A. W. (2024). Adsorption of metal porphyrins using chitosan/zeolite-X composite as an efficient demetallization agent for crude oil: Isotherm, kinetic, and thermodynamic studies. *International Journal of Biological Macromolecules*, *274*(P1), 133358. https://doi.org/10.1016/j.ijbiomac.2024.133358
39. Medina, O. E., Galeano-Caro, D., Villada, Y. V., Perez-Cadenas, A. F., Carrasco-Marín, F., Franco, C. A., Corteś, F. B. (2023). Regeneration/reuse capability of monolithic carbon xerogels-metal nanocomposites for crude oil removal from oil-in-saltwater emulsions. In: *Nanotechnology for Oil-Water Separation: From Fundamentals to Industrial Applications*. https://doi.org/10.1016/B978-0-323-95517-1.00013-5
40. Megersa, N., Legessea, A., Getachew, H., Mulatu, A., Kebede, T. (2025). Biosorbent residues of the traditionally fermented ethiopian honey wine (tej) for quantitative removal of heavy metals from contaminated waters: adsorption kinetics, thermodynamics and equilibrium studies. *Scientific African*, e02821. https://doi.org/10.1016/j.sciaf.2025.e02821
41. Narayana, P. L., Maurya, A. K., Wang, X. S., Harsha, M. R., Srikanth, O., Alnuaim, A. A., Hatamleh, W. A., Hatamleh, A. A., Cho, K. K., Paturi, U. M. R., Reddy, N. S. (2021). Artificial neural networks modeling for lead removal from aqueous solutions using iron oxide nanocomposites from bio-waste mass. *Environmental Research*, *199*, 111370. https://doi.org/10.1016/j.envres.2021.111370
42. Naushad, M., Ahamad, T., AlOthman, Z. A., Al-Muhtaseb, A. H. (2019). Green and eco-friendly nanocomposite for the removal of toxic Hg(II) metal ion from aqueous environment: Adsorption kinetics & isotherm modelling. *Journal of Molecular Liquids*, *279*, 1–8. https://doi.org/10.1016/j.molliq.2019.01.090
43. Obaid, A. O., Al Zbedy, A. S., Alrashdi, K. S., Aljohani, M. M., Alqarni, S. A., Al-Bonayan, A. M., Abumelha, H. M., El-Metwaly, N. M. (2025). Mercury capture using functionalized metal-organic framework encapsulated in dual hydrogel layers of β-cyclodextrin and polyethylenimine: Synthesis, characterization, adsorption, thermodynamics, and Box–Behnken design analysis. *Carbohydrate Polymer Technologies and Applications*, *10*, 100793. https://doi.org/10.1016/j.carpta.2025.100793
44. Owoeye, S. S., Jegede, F. I., Borisade, S. G. (2020). Preparation and characterization of nano-sized silica xerogel particles using sodium silicate solution extracted from waste container glasses. *Materials Chemistry and Physics*, *248*, 122915. https://doi.org/10.1016/j.matchemphys.2020.122915
45. Pandey, G., Rajput, N. S., Sharma, U. K., Chauhan, M. S., Lamba, N. P. (2025). Remediation of environmental issues using graphene based materials for water purification: Synthesis, kinetics, and factors effecting the removal of heavy metal ions. *Next Materials*, *8*, 100765. https://doi.org/10.1016/j.nxmate.2025.100765
46. Pilato, L. D., Baieli, M. F., Miranda, M. V., Sapag, K., Copello, G. J., Wolman, F. J. (2025). Induced porosity in chitin xerogels for use in protein adsorption and purification. *Materials Chemistry and Physics*, *339*, 130706. https://doi.org/10.1016/j.matchemphys.2025.130706
47. Rahman, M. L., Shamrih, S. A., Azlyzan, N. A., Sarjadi, M. S., Arsad, S. E., Sarkar, S. M., Kumar, S. (2025). Removal of heavy metal ions from wastewater using modified cornstalk cellulose-derived poly(amidoxime) ligand. *Carbohydrate Polymer Technologies and Applications*, *9*, 100633. https://doi.org/10.1016/j.carpta.2024.100633
48. Riyanto, A., Machmudah, S., Purwaningsih, S. Y., Pratapa, S. (2025). Rice husk-based silica: A structural and optical study of xerogel, amorphous, and crystalline phases. *Optical Materials*, *166*(April), 117115. https://doi.org/10.1016/j.optmat.2025.117115
49. Sarkar, S., Mondal, N. K. (2024). Preparation of low-cost metal-loaded adsorbent using post-consumer

waste plastics: Experimental and modelling studies. *Environmental Nanotechnology, Monitoring and Management*, *22*, 101009. https://doi.org/10.1016/j.enmm.2024.101009

50. Scherdel, C., Reichenauer, G. (2015). Highly porous silica xerogels without surface modification. *Journal of Supercritical Fluids*, *106*, 160–166. https://doi.org/10.1016/j.supflu.2015.08.016
51. Shi, C., Niu, F., Xie, Y., Zhang, Z., Geng, J., Wang, C. (2025). Mechanism of dynamic interaction between aging microplastics and heavy metal ions under different hydrodynamic environments. *Journal of Water Process Engineering*, *71*, 107232. https://doi.org/10.1016/j.jwpe.2025.107232
52. Shoppert, A., Valeev, D., Loginova, I., Chaikin, L. (2020). Complete extraction of amorphous aluminosilicate from coal fly ash by alkali leaching under atmospheric pressure. *Metals 10*(12). https://doi.org/10.3390/met10121684
53. Soroceanu, A., Stiubianu, G. T. (2021). Siloxane matrix molecular weight influences the properties of nanocomposites based on metal complexes and dielectric elastomer. *Materials 14*(12). https://doi.org/10.3390/ma14123352
54. Souto, F. T., Machado, V. G. (2023). Hybrid films composed of ethyl(hydroxyethyl)cellulose and silica xerogel functionalized with a fluorogenic chemosensor for the detection of mercury in water. *Carbohydrate Polymers*, *304*, 120480. https://doi.org/10.1016/j.carbpol.2022.120480
55. Srivastava, S., Kumar, V., Singh, S. K., Yadav, P., Singh, B., Bhaskar, A. (2024). A review on application of artificial intelligence in mechanical engineering. *Machine Learning Techniques and Industry Applications*, *323*, 29–46. https://doi.org/10.4018/979-8-3693-5271-7.ch002
56. Taleb, M. A., Kumar, R., Barakat, M. A., Almeelbi, T., Seliem, M. K., Ahmad, A. (2024). Recent advances in heavy metals uptake by tailored silica-based adsorbents. *Science of the Total Environment*, *955*, 177093. https://doi.org/10.1016/j.scitotenv.2024.177093
57. Tan, N., Xie, T., Hu, P., Feng, Y., Li, Q., Zhao, S., Zhou, H., Zeng, W., Zeng, J. (2021). *Preparation and characterization of capric-palmitic acids eutectics / silica xerogel / exfoliated graphite nanoplatelets form-stable phase change materials*. *34*. https://doi.org/10.1016/j.est.2020.102016
58. Thommes, M., Kaneko, K., Neimark, A. V., Olivier, J. P., Rodriguez-Reinoso, F., Rouquerol, J., Sing, K. S. W. (2015). Physisorption of gases, with special reference to the evaluation of surface area and pore size distribution (IUPAC Technical Report). *Pure and Applied Chemistry*, *87*(9–10), 1051–1069. https://doi.org/10.1515/pac-2014-1117
59. Tran, G. H., Leu, H. J., Richards, D., Lo, S. S., Tran, T. T. (2025). Biosynthesis and application of biological thin films for heavy metal ion biosorption from aqueous solution. *Journal of Environmental Chemical Engineering*, *13*(1), 115014. https://doi.org/10.1016/j.jece.2024.115014
60. Vareda, J. P., Valente, A. J. M., Durães, L. (2020). Silica aerogels/xerogels modified with nitrogen-containing groups for heavy metal adsorption. *Molecules 25*(12). https://doi.org/10.3390/molecules25122788
61. Wang, C., Xu, G., Gu, X., Gao, Y., Zhao, P. (2021). High value-added applications of coal fly ash in the form of porous materials: A review. *Ceramics International*, *47*(16), 22302–22315. https://doi.org/10.1016/j.ceramint.2021.05.070
62. Wang, P., Du, M., Zhu, H., Bao, S., Yang, T., Zou, M. (2015). Structure regulation of silica nanotubes and their adsorption behaviors for heavy metal ions: PH effect, kinetics, isotherms and mechanism. *Journal of Hazardous Materials*, *286*, 533–544. https://doi.org/10.1016/j.jhazmat.2014.12.034
63. Wang, R., Ng, D. H. L., Liu, S. (2019). Recovery of nickel ions from wastewater by precipitation approach using silica xerogel. *Journal of Hazardous Materials*, *380*, 120826. https://doi.org/10.1016/j.jhazmat.2019.120826
64. Yan, F., Liu, Y., Wang, H., Zhang, M., Guo, M. (2023). Amino-terminated SiO_2–Al_2O_3 composite aerogels from fly ash for improved removal of Cu^{2+} and Pb^{2+} ions in wastewater: one-pot synthesis, excellent adsorption capacity and mechanism. *Environmental Science and Pollution Research*, *30*(9), 23655–23667. https://doi.org/10.1007/s11356-022-23775-2
65. Yang, B. T., Lin, Y. F., Chen, C. C. (2024). Greener production of high-performance silica xerogel: Upcycling waste glass using deep eutectic solvent-assisted extraction of residual Na^+. *Journal of Cleaner Production*, *448*, 141401. https://doi.org/10.1016/j.jclepro.2024.141401
66. Yücel, S., Karakuzu, B., Terzioğlu, P., Temel, T. M. (2016). Influence of gel aging time on the properties of various silica aerogels synthesized from water glass. *Materials Science Forum*, *866*, 176–180. https://doi.org/10.4028/www.scientific.net/MSF.866.176
67. Zheng, C., Hu, D., Liu, Z., Zhang, X., Yu, K., Ma, W. (2024). A simple and efficient in situ polymerization of silica xerogel-acrylic thermal insulation coatings. *Progress in Organic Coatings*, *187*, 108142. https://doi.org/10.1016/j.porgcoat.2023.108142
68. Zheng, Q., Dong, L., Shen, P., Liu, D. (2025). A novel activation scheme for fine cassiterite flotation by using a metal ion modified collector. *Colloids and Surfaces A: Physicochemical and Engineering Aspects*, *710*, 136310. https://doi.org/10.1016/j.colsurfa.2025.136310
69. Zhou, G., Wang, Q., Wei, B., Xin, S., Yang, W., Shao, W. (2025). Surfactant enhanced amine-based silica for coal wetting: Organic surface modification and synergistic mechanism. *Journal of Environmental Chemical Engineering, 13*(5), 117761. https://doi.org/10.1016/j.jece.2025.117761